

Purely electronic terahertz polarization in dimer Mott insulators

Hiroki Gomi,^{1,2} Takayuki Imai,¹ Akira Takahashi,^{1,2} and Masaki Aihara¹

¹Graduate School of Materials Science, Nara Institute of Science and Technology, Ikoma, 630-0192, Japan

²CREST, Japan Science and Technology Agency, Chiyoda-ku, Tokyo 102-0075, Japan

(Received 27 April 2010; revised manuscript received 3 June 2010; published 1 July 2010)

We theoretically describe purely electronic polarization modes in terahertz frequency region in dimer Mott insulators κ -(BEDT-TTF)₂X. The unusual low-frequency modes arise from the coupling between the oscillation of intradimer electric dipole moments and that of alternating interdimer bond orders. These collective modes play an important role in the dynamical dielectric properties of the dimer Mott insulators. Near the phase boundary of the dimer Mott transition, the ferroelectric ground state is realized by introducing electron-lattice coupling as a result of the softening of one of these collective modes.

DOI: 10.1103/PhysRevB.82.035101

PACS number(s): 71.30.+h, 77.80.-e, 78.30.Jw

I. INTRODUCTION

Low-dimensional strongly correlated electron systems with a quarter-filled band have recently attracted much attention. BEDT-TTF salts are typical two-dimensional systems with anisotropic triangular lattices, and the strong correlation and frustration act cooperatively to generate exotic phases. Among the BEDT-TTF salts, κ -(BEDT-TTF)₂X (X: a counter anion) exhibit the Mott insulator phase,¹⁻⁵ the exotic superconducting phase,⁶ the spin liquid phase,⁷⁻⁹ and so on. The BEDT-TTF molecular lattice is distorted to form dimers in κ -(BEDT-TTF)₂X. Hybridized two sites can be effectively treated as a single site, and the valence band is regarded as a half-filled one. As a result, κ -(BEDT-TTF)₂X exhibits the Mott insulator phase if the effective on-site Coulomb energy is large enough. The state is called the dimer Mott insulator.

Recently quite interesting charge excitation phenomena have been observed in the dimer Mott insulators: the photo-induced phase transition to a metallic state,¹⁰ and the dielectric anomaly, where a broad peak has been observed around 25 K in the temperature dependence of the dielectric constant.¹¹ In particular, the latter suggests that low-energy charge excitation exists in the dimer Mott insulators in contrast to the case of the Mott insulators.

In this paper, we show that the dimer Mott insulator has terahertz electric polarization, which purely arises from the electron dynamics. The ferroelectricity which arises from the electron dynamics has been observed in some materials, and these ferroelectrics have unconventional origins such as charge order generation.¹²⁻¹⁷ We propose another origin of ferroelectricity in this paper.

II. METHOD OF CALCULATION

We adopt the 1/4-filled extended Hubbard Hamiltonian for holes on the two-dimensional anisotropic triangular lattice, which includes the degrees of freedom in a dimer. It is given by

$$H = \sum_{\langle n,m \rangle} (\beta_{n,m} \hat{p}_{n,m} + V_{n,m} n_n n_m) + U \sum_n n_{n,\uparrow} n_{n,\downarrow}, \quad (1)$$

where $\langle n,m \rangle$ denotes the neighbor site pairs, $c_{n,\sigma}$ ($c_{n,\sigma}^\dagger$) is the annihilation (creation) operator for a hole of spin σ at the site

n , $\beta_{n,m}$ ($V_{n,m}$) is the transfer integral (the Coulomb interaction energy) between the sites n and m , $\hat{p}_{n,m} = \sum_\sigma (c_{m,\sigma}^\dagger c_{n,\sigma} + c_{n,\sigma}^\dagger c_{m,\sigma})$, U is the on-site Coulomb interaction energy, $n_{n,\sigma} = c_{n,\sigma}^\dagger c_{n,\sigma}$, and $n_n = \sum_\sigma n_{n,\sigma}$.

We calculate the quantum state excited by light pulse expressed by the vector potential with a Gaussian profile. The vector potential at time t is given by

$$A(t) = eA \exp(-(t/D)^2) \cos(\omega_p t), \quad (2)$$

where A is the maximum amplitude, D is the duration time, ω_p is the center frequency, and e is the unit polarization vector. We consider the one-photon excited states in this paper. The electron-light interaction Hamiltonian of the first order in A is given by

$$H_{e-1}(t) = -A(t) \cdot \hat{J}, \quad (3)$$

where \hat{J} is the current operator, and it is given by

$$\hat{J} = i \sum_{\langle n,m \rangle, \sigma} (\mathbf{m} - \mathbf{n}) \beta_{n,m} (c_{n,\sigma}^\dagger c_{m,\sigma} - c_{m,\sigma}^\dagger c_{n,\sigma}), \quad (4)$$

and \mathbf{n} is the position vector of the site n . The position vectors are determined with using the following parameters:¹⁸ the lattice constant along the a axis $a = 12.9$ Å, that along the c axis $c = 8.4$ Å, the dihedral angle between the molecular planes $\theta = 92.3^\circ$, the inclination angle of molecular long axis $\delta = 34.0^\circ$ from the direction perpendicular to the conducting sheet, and the distance $l = 3.56$ Å between the molecules in a dimer. We adopt the atomic units, where the light velocity, the elementary electric charge, and \hbar are equal to 1.

To the first order in A , the solution $|\psi(t)\rangle$ of the Schrödinger equation subject to the pulse is given by

$$|\psi(t)\rangle = |\psi_0\rangle + |\psi^{(1)}(t)\rangle, \quad (5)$$

where $|\psi_0\rangle$ is the ground state of H , and

$$|\psi^{(1)}(t)\rangle = i \int_{-\infty}^t dt' \exp(-iH(t-t')) A(t') \cdot \hat{J} |\psi_0\rangle. \quad (6)$$

Here and hereafter, we set the reference of energy so that the energy eigenvalue for the ground state E_0 is zero. The ground state $|\psi_0\rangle$ and the first-order solution $|\psi^{(1)}(t)\rangle$ are, respec-

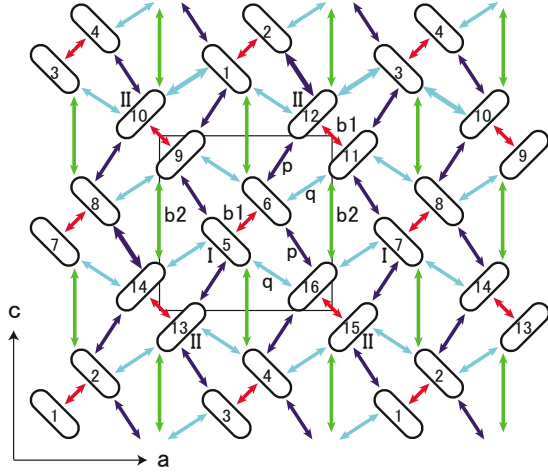


FIG. 1. (Color online) Anisotropic triangular lattices for κ -(BEDT-TTF) $_2$ X. The site numbers for the periodic boundary condition I are shown.

tively, calculated exactly by the Lanczos method and by solving Eq. (6) numerically.

We consider the first-order changes of the charge density $\rho_n^{(1)}(t)$, the bond order $p_{n,m}^{(1)}(t)$, and the spin correlation function $\eta_{n,m}^{(1)}$ induced by the pulse excitation. They are given by

$$\rho_n^{(1)}(t) = (\langle \psi_0 | n_n | \psi^{(1)}(t) \rangle + \text{c.c.}) / A, \quad (7)$$

$$p_{n,m}^{(1)}(t) = (\langle \psi_0 | \hat{p}_{n,m} | \psi^{(1)}(t) \rangle + \text{c.c.}) / A, \quad (8)$$

$$\eta_{n,m}^{(1)} = (\langle \psi_0 | \mathbf{S}_n \cdot \mathbf{S}_m | \psi^{(1)}(t) \rangle + \text{c.c.}) / A, \quad (9)$$

where \mathbf{S}_n is the spin operator at the site n . Since the absolute value of the bond order shows the strength of the bond, we define the difference in the absolute value of the bond orders between $|\psi(t)\rangle$ and $|\psi_0\rangle$ as

$$|p_{n,m}^{(1)}(t)| = |\bar{p}_{n,m} + p_{n,m}^{(1)}(t)| - |\bar{p}_{n,m}|, \quad (10)$$

where $\bar{p}_{n,m}$ is the bond order for the ground state. The bond is stronger in $|\psi(t)\rangle$ than in $|\psi_0\rangle$ for $|p_{n,m}^{(1)}(t)| > 0$.

III. RESULTS

As shown in Fig. 1, there are four nonequivalent bonds, and they are labeled by b1, b2, p, and q according to Mori *et al.*¹⁸ We use the 4×4 cluster of the system size $N=16$ with three different periodic boundary conditions. In the periodic boundary condition I (II), the 16-site clusters are tiled in a staggered manner along the a axis (c axis) to cover the anisotropic triangular lattice. In the condition III, the clusters are tiled without staggering. We mainly use the condition I shown in Fig. 1, because interdimer networks of important p and b1 bonds are the longest in the case. The influence of the periodic boundary condition on the results will be mentioned later.

The b1 bond is much stronger than the other ones, and the two BEDT-TTF molecules connected by the b1 bond form a dimer. There are two dimers in the unit cell, and they are labeled by I and II as shown in Fig. 1. The transfer integral

β_{b1} and V_{b1} denote $\beta_{n,m}$ and $V_{n,m}$ for the b1 bond, respectively, and the others are denoted in the same way. The values of the transfer integrals for κ -(BEDT-TTF) $_2$ Cu[N(CN) $_2$]Br are calculated by the extended Hückel method,¹⁸ and they are given by, $\beta_{b1} = 0.265$ eV, $\beta_{b2} = 0.098$ eV, $\beta_p = 0.109$ eV, and $\beta_q = -0.038$ eV. The value of U is estimated to be 0.7 eV from the Knight shift.^{19,20} As for the Coulomb interaction energies between the neighbor sites, the estimated values are 0.27 eV \sim 0.35 eV in the cases of α -(BEDT-TTF) $_2$ I $_3$ and θ -(BEDT-TTF) $_2$ RbZn(SCN) $_4$ without dimerization.^{21,22} It is expected that V_{b1} is larger, and V_{b2} , V_p , and V_q are smaller than these values in the dimerized present case.

A. Ground state

To estimate the reasonable parameters for κ -(BEDT-TTF) $_2$ X, we calculate the ground state $|\psi_0\rangle$ in the wide ranges of parameter space. To investigate the physical properties of $|\psi_0\rangle$, we numerically calculate the charge density $\bar{\rho}_n = \langle \psi_0 | n_n | \psi_0 \rangle$, the charge correlation function $\bar{\xi}_{n,m} = \langle \psi_0 | n_n n_m | \psi_0 \rangle$, the spin correlation function $\bar{\eta}_{n,m} = \langle \psi_0 | \mathbf{S}_n \cdot \mathbf{S}_m | \psi_0 \rangle$, and the probability W_s that a dimer is singly occupied in $|\psi_0\rangle$. We first calculate the U and V_{b1} dependence of these quantities in the range 0.25 eV $< V_{b1} < U < 0.75$ eV fixing the other parameters. We fix V_{b2} , V_p , and V_q to 0.25 eV. As for the values of transfer integrals, the values obtained from the extended Hückel calculation are used. Here and hereafter these values of transfer integrals are used unless the values are explicitly mentioned. There are three phases, and these physical quantities discontinuously change at the two phase boundary lines in the U - V_{b1} plane. We denote the larger critical value of V_{b1} for a given U by $V_{b1}^1(U)$ and smaller one by $V_{b1}^2(U)$. For $V_{b1} > V_{b1}^1(U)$, the spin correlation is always negative between the dimers I and II, showing that the ground state is an antiferromagnetic (AFM) state. Furthermore, $W_s \geq 0.86$ holds all through the AF ground state region. For $V_{b1}^1(U) > V_{b1} > V_{b1}^2(U)$, and for $V_{b1} < V_{b1}^2(U)$, the spin correlations are much smaller than those for the AFM ground state, showing that the ground state is a paramagnetic (PM) state. Both $V_{b1}^1(U)$ and $V_{b1}^2(U)$ increase with decreasing U . For example, $V_{b1}^1(U) = 0.59$ eV at $U = 0.75$ eV, and $V_{b1}^2(U) = 0.25$ eV at $U = 0.60$ eV. The PM phase for $V_{b1} < V_{b1}^2(U)$ exists in the unrealistic parameter region, and we focus on the AFM state and the PM state for $V_{b1}^1(U) > V_{b1} > V_{b1}^2(U)$ in the following.

As for the charge structures of the AFM and the PM states, the charge density is uniform, and the charge order is not formed as seen from the charge correlation functions for the two states.

Both a dimer Mott insulator in a spin liquid state and a metallic state have PM spin correlation. To see the physical properties of the PM state, we also investigate the β_{b1} dependence of these physical quantities fixing all the other parameters. We set $U = 0.7$ eV, $V_{b1} = 0.45$ eV, $V_{b2} = V_p = V_q = 0.25$ eV. Decreasing β_{b1} , the PM ground state changes continuously as β_{b1} is decreased even to the value of β_{b2} or β_p . This shows that the PM state is stable without dimerization, and therefore it is not a dimer Mott insulator in a spin

liquid state. Furthermore, W_s decreases continuously to about 0.5 as β_{b1} is decreased. These results strongly suggest that the AFM state is a dimer Mott insulator, and the PM state is metallic.

We also investigate the V_p dependence of $\bar{\rho}_n$, $\bar{\xi}_{n,m}$, $\bar{\eta}_{n,m}$, and W_s for $|\psi_0\rangle$. We set $U=0.7$ eV, $V_{b1}=0.45$ eV, $V_{b2}=V_q=0.25$ eV. For $V_p \leq 0.35$ eV, the ground state is the PM state. For $V_p \geq 0.36$ eV, the ground state is a charge ordered state, where there is charge disproportion between the dimer I and II. It is estimated that the point charge relation $V_x \propto r_x$ approximately holds, where r_x is the distance between the centers of two molecules connected by the x bond, in $(\text{BEDT-TTF})_2X$.²³ Between the interdimer p , $b2$ and q bonds, r_p (r_q) is the shortest (longest), and $r_q/r_p=1.20$ holds.¹⁸ Therefore, the parameter region where the charge order appears is also unrealistic.

Consequently, in the realistic parameter region, the ground state is either the AFM dimer Mott insulator or the PM metal, and the phase transition between them occurs by changing various parameters. This result is consistent with previous ones where the U dependence of $|\psi_0\rangle$ is investigated within the Hartree-Fock approximation.^{19,20} In this paper, we show the β_{b2} dependence of various physical quantities because the spin frustration can be controlled by changing β_{b2} , with using the following fixed parameters: $U=0.7$ eV, $V_{b1}=0.45$ eV, $V_{b2}=V_p=V_q=0.25$ eV. The ground state is the AFM dimer Mott insulator for $\beta_{b2} \leq 0.073$ eV, and it is the PM metal for $\beta_{b2} \geq 0.074$ eV. The physical properties of these AFM and PM states are basically unchanged in the realistic parameter range, and essentially the same results are obtained.

B. Light absorption spectrum

The properties of the optically excited states are typically reflected in the light absorption spectrum. In this paper, we focus our attention to the unconventional light absorption in the terahertz frequency region in dimer Mott insulators. In Fig. 2, we show the β_{b2} dependence of light absorption spectrum $\alpha(\omega)$ in the energy region $\omega \leq 0.1$ eV. The dominant peaks in $\alpha(\omega)$ are in the region $\omega \geq 0.2$ eV. In addition to these large peaks, there are much smaller peaks in the region both in the cases of light excitation from the AFM and the PM ground states. The existence of these low-energy modes is not restricted to a special parameter region. In the realistic parameter regions, the excitation energies are always in the terahertz region near the phase boundary of the Mott transition. It should be emphasized that such low energy peaks are not observed in the simple Mott and charge ordered insulators.

We next show the time dependence of the physical quantities induced by a terahertz light pulse. In all the following cases, the center frequency ω_p of the pulse is chosen to be resonant to the largest peak in the energy region shown in Fig. 2. The used duration time $D=100$ eV⁻¹ is large enough that the contributions from the large peaks in the higher energy region are negligible.

C. Photoexcited mode from AFM ground state

In this subsection, we show the results in the case of the AFM ground state. We first show the results when the light is

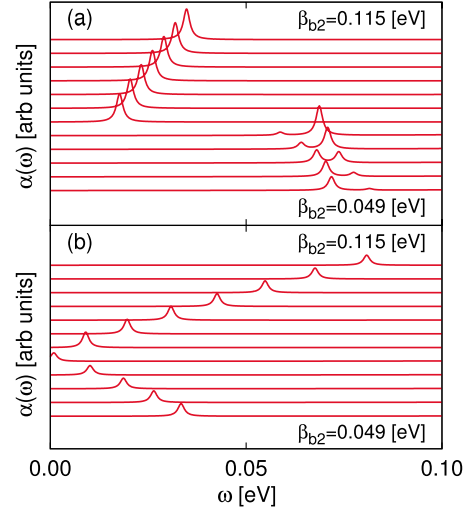


FIG. 2. (Color online) Light absorption spectrum $\alpha(\omega)$ when the light is polarized (a) to the a direction and (b) to the c direction for various values of β_{b2} . The interval of β_{b2} is 0.006 eV. The artificial broadening factor of 0.001 eV is used.

polarized to the c axis. In Fig. 3, we show the time dependence of charge and bond order changes induced by the terahertz light at $\beta_{b2}=0.069$ eV. The $b1$, $b2$, p , and q bonds are shown by the red, the green, the dark blue, and the light blue lines, respectively, in Fig. 3(a). Moreover, there are two nonequivalent p (q) bonds with different bond orders in the photoexcited state $|\psi(t)\rangle$. These two nonequivalent bonds are distinguished by the solid and the dashed lines. Two sites forming a dimer also become nonequivalent in $|\psi(t)\rangle$, and they are distinguished by the solid red and the dashed green ellipsoids. We show $\rho_n^{(1)}(t)$ and $|p|_{n,m}^{(1)}(t)$ in Figs. 3(b) and 3(c), respectively, for the sites and the bonds shown in Fig. 3(a). As seen from these figures, $\rho_n^{(1)}(t)$ and $|p|_{n,m}^{(1)}(t)$ oscillate coherently. We choose the sites and the bonds shown by the solid and dashed lines so that the quantities at the sites and the bonds shown by the same (different) kinds of lines oscillate in (out of) phase.

Before analyzing the present results, we introduce bond order alternation between dimers in much simpler one-dimensional quarter-filled electron-lattice coupled systems. The dimer Mott insulator with alternating bond lengths and bond orders between the dimers is schematically shown in Fig. 4. The site connected by the stronger bond becomes charge-rich because electrons are more stabilized on the stronger bond. The state becomes the ground state with the deformed lattice in a parameter range.²⁴⁻²⁶

The collective motion induced by the terahertz light pulse can be regarded as the bond order alternation between the dimers. As seen from Fig. 3(c), the amplitudes of the induced bond order oscillation for the p and q bonds are much larger than those for the other bonds, and therefore we focus on the p and q bonds. As seen from Fig. 3(a), the interdimer bond orders for the p and q bonds alternate along the a direction, and the amplitude of the alternation oscillates in time. Since charges are attracted by stronger bonds, when the bonds shown by the solid (dashed) lines become stronger, the sites shown by the solid red (dashed green) ellipsoids, each of

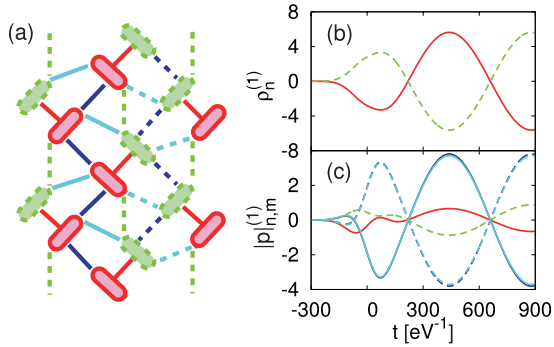


FIG. 3. (Color) The charge and bond order changes induced by the light polarized along the c direction for $\beta_{b2}=0.069$ eV. (a) Nonequivalent bonds and sites are distinguished by the colors and the kinds (solid or dashed) of lines. (b) $\rho_n^{(1)}(t)$ and (c) $|p_{n,m}^{(1)}(t)|$ are shown by the lines of the colors and the kinds that specify the site n and the bond $\langle n,m \rangle$, respectively, in (a).

which is connected by two stronger p bonds, become charge-rich as seen from Figs. 3(b) and 3(c). In this way, the bond order and the charge density oscillations are strongly coupled in the collective mode. The mode corresponds a photoinactive covalent mode in the model where the electric degrees of freedom in a dimer are not included. The low-energy covalent mode becomes photoactive as a result of this unique coupling. The excitation induces the polarization along the c direction due to the collective electric dipole moment on each dimer.

As for the interdimer spin correlations, $-\eta_{n,m}^{(1)}$ are roughly proportional to $|p_{n,m}^{(1)}(t)|$, showing that when a bond order becomes stronger, the AF spin correlation for the bond becomes stronger. This holds all the cases shown in the following. Therefore, the collective mode can be regarded as a kind of spin-Peierls mode.

It should be emphasized that the lattice deformation is not considered here. In the previous works about the one-dimensional systems, interdimer bond order alternation occurs as a result of electron-lattice coupling. On the other hand, in the present case, the induced collective motion of the bond order alternation coupled with polarization has purely electronic origin. We have found this purely electronic low-energy excitation also in the one-dimensional dimer Mott insulators. Since the electron-lattice coupling is strong in κ -(BEDT-TTF) $_2$ X, this collective mode and the phonon modes may be strongly coupled. This point will be discussed later.

We next show the results when the light is polarized to the a axis. In Fig. 5, we show the time dependence of charge and bond order changes induced by the light at $\beta_{b2}=0.069$ eV. As seen from Fig. 5(c), the amplitudes of the induced bond



FIG. 4. (Color online) The schematic representation of bond order alternation between dimers. The ellipsoids represent the dimers, and the solid (dashed) lines show the stronger (weaker) bonds connecting the dimers. The solid (dashed) circles represent the charge-rich (charge-poor) sites.

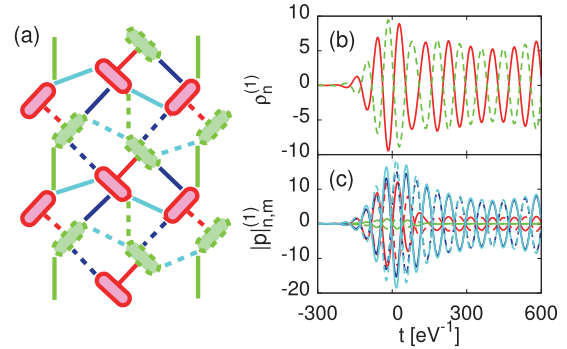


FIG. 5. (Color) The charge and bond order changes induced by the light polarized along the a direction for $\beta_{b2}=0.069$ eV. (a) Nonequivalent bonds and sites are distinguished by the colors and the kinds (solid or dashed) of lines. (b) $\rho_n^{(1)}(t)$ and (c) $|p_{n,m}^{(1)}(t)|$ are shown by the lines of the colors and the kinds that specify the site n and the bond $\langle n,m \rangle$, respectively, in (a).

order oscillation for the p and q bonds are much larger than those for the other bonds in the time region $t \gtrsim 200$ where the pump pulse has almost gone off. As seen from Fig. 5(a), the bond orders for p and q bonds alternate along the c direction. The bond order and the charge density oscillations are strongly coupled in the collective mode just like the case of c direction excitation, and the low-frequency electric polarization along the a direction is induced by the excitation.

D. Photoexcited mode from PM ground state

In this subsection, we show the results in the case of the PM ground state. We first show the results when the light is polarized to the c axis. In Fig. 6, we show the time dependence of charge and bond order changes induced by the light at $\beta_{b2}=0.098$ eV. As seen from this figure, the amplitudes of the induced bond order oscillation for the p and q bonds are much larger than those for the other bonds, and the bond orders for p and q bonds alternate along the a direction. The bond order and the charge density oscillations are strongly coupled in the collective mode, and the electric polarization

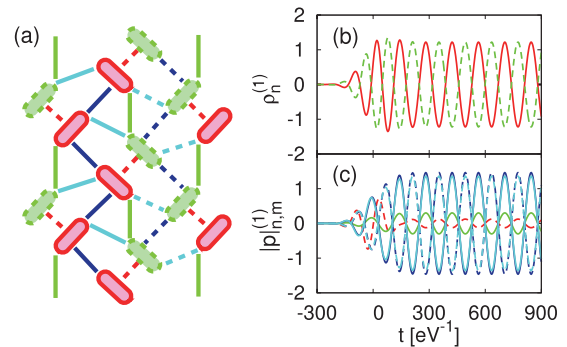


FIG. 6. (Color) The charge and bond order changes induced by the light polarized along the c direction for $\beta_{b2}=0.098$ eV. (a) Nonequivalent bonds and sites are distinguished by the colors and the kinds (solid or dashed) of lines. (b) $\rho_n^{(1)}(t)$ and (c) $|p_{n,m}^{(1)}(t)|$ are shown by the lines of the colors and the kinds that specify the site n and the bond $\langle n,m \rangle$, respectively, in (a).

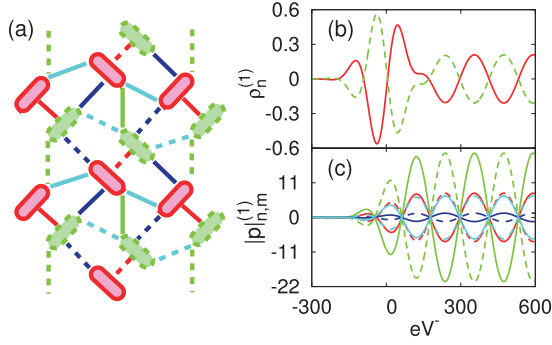


FIG. 7. (Color) The charge and bond order changes induced by the light polarized along the a direction for $\beta_{b2}=0.098$ eV. (a) Nonequivalent bonds and sites are distinguished by the colors and the kinds (solid or dashed) of lines. (b) $\rho_n^{(1)}(t)$ and (c) $|p|_{n,m}^{(1)}(t)$ are shown by the lines of the colors and the kinds that specify the site n and the bond $\langle n,m \rangle$, respectively, in (a).

along the c direction is induced just like the c -axis excitation case of the AFM ground state.

We next show the results when the light is polarized to the a axis. In Fig. 7, we show the time dependence of charge and bond order changes induced by the light at $\beta_{b2}=0.098$ eV. As seen from this figure, the amplitude of the induced oscillation for the b2 bonds is the largest between the bonds in this case, and it is much larger than the largest ones in the other cases. However, the induced dipole moment is much smaller in this case compared with the other cases. This can be understood as follows. As seen from Fig. 7(a), a dimer is connected by two solid b2 bonds or two dashed b2 bonds. The dominant motion of the b2 bonds does not accompany the bond order alternation between the dimers, and the coupling with the charge motion is very weak.

Finally we comment on the effects of periodic boundary conditions. Qualitatively the same results are obtained with using the condition III, but the peaks in the light absorption spectrum almost disappear when the light is polarized to the a -axis, with using the condition II. Finite size effects are not negligible in the present results.

E. Ferroelectric ground state

As mentioned in Sec. III A, neither the ferroelectric nor charge ordered phase is obtained within the present model in the realistic parameter region. However, the ground state becomes ferroelectric by introducing electron-lattice coupling near the phase boundary of the Mott transition. For example, if the dimers denoted by I (II) in Fig. 1 shift to left (right) by $\delta r/2$, then the transfer integral for the x ($x=p$ or q) bonds shown by the solid lines in Fig. 3(a), is different from that shown by the dashed lines. We denote the x bonds shown by the solid (dashed) lines by the xs (xd) bonds. In the small δr limit, the transfer integrals are given by

$$\beta_{ps} = \beta_p + \Delta,$$

$$\beta_{pd} = \beta_p - \Delta,$$

$$\beta_{qs} = \beta_q + s\Delta,$$

$$\beta_{qd} = \beta_q - s\Delta, \quad (11)$$

where $\Delta = \beta'_p \delta r$, β'_x is the electron-lattice coupling for the x bonds, and $s = \beta'_q / \beta'_p$.

We define the state $|\psi_1\rangle$ by

$$|\psi_1\rangle = \langle \psi^{(1)}(\tau) | \psi^{(1)}(\tau) \rangle^{-1/2} | \psi^{(1)}(\tau) \rangle. \quad (12)$$

Here we consider the case when the light is polarized to the c direction, and $|p|_{n,m}^{(1)}(t)$ for the bonds shown by the solid lines become maximum at $t = \tau$ after the pump pulse has gone off. For example $\tau = 442$ eV $^{-1}$ in the case of Fig. 3. Since $|\Delta\epsilon|D > 10$, where $\Delta\epsilon$ is the difference in the peak energy from the nearest peak, $|\psi_1\rangle$ is the energy eigenstate responsible to the absorption peak in the terahertz frequency region.

We consider the hybridized state of $|\psi_0\rangle$ and $|\psi_1\rangle$ given by

$$|\psi\rangle = \sqrt{1 - C_1^2} |\psi_0\rangle + C_1 |\psi_1\rangle, \quad (13)$$

where C_1 is a real constant. The bond orders for xs and xd bonds for $|\psi\rangle$ are given by

$$p_{xs} = \bar{p}_x (1 - C_1^2) + p'_x C_1 \sqrt{1 - C_1^2} + (1/2) p''_x C_1^2, \quad (14)$$

$$p_{xd} = \bar{p}_x (1 - C_1^2) - p'_x C_1 \sqrt{1 - C_1^2} + (1/2) p''_x C_1^2, \quad (15)$$

where $\bar{p}_x = \langle \psi_0 | \hat{p}_{n,m} | \psi_0 \rangle$, $p'_x = \langle \psi_0 | \hat{p}_{n,m} | \psi_1 \rangle + \text{c.c.}$, $p''_x = 2 \langle \psi_1 | \hat{p}_{n,m} | \psi_1 \rangle$, and $\langle n,m \rangle$ is the site pair of the xs bond. The energy expectation value for $|\psi\rangle$ with the distorted lattice minus the ground state energy E_0 without lattice distortion is given by

$$\Delta E(C_1, \Delta) = \alpha C_1^2 + \beta C_1 \Delta + \gamma \Delta^2, \quad (16)$$

to the second order in C_1 and Δ . Here $\alpha = E_1 - E_0$, E_1 is the energy eigenvalue for $|\psi_1\rangle$, $\beta = N_p (p'_p + s p'_q)$, N_p is the number of p or q bonds, $\gamma = N_p (1/2) (K_p / (\beta'_p)^2 + s^2 K_q / (\beta'_q)^2)$, and K_x is the spring constant for x bond. The energy difference ΔE is minimized when $C_1 = -\beta / (2\alpha)\Delta$ and then

$$\Delta E = [\gamma - \beta^2 / (4\alpha)] \Delta^2. \quad (17)$$

Therefore, when $\alpha < \beta^2 / (4\gamma)$, lattice distortion occurs and $|\psi_1\rangle$ is hybridized to $|\psi_0\rangle$. Since the hybridized state is equivalent to $|\psi(\tau)\rangle$ to the first order of $C_1 \propto \Delta$, the ground state has a finite electric polarization in the small Δ case. We confirm by a numerical calculation that the ground state has a finite polarization arising from an electric dipole on a dimer when the transfer integrals of p , q , or both bonds are given by Eq. (11) with small Δ .

It is estimated that $(\beta'_x)^2 / K_x \sim 0.06$ eV for b2 bond of α -(BEDT-TTF) $_2$ I $_3$.²² Since the transfer integral depends on the relative position of the two molecules in a very complicated way, the values for the p and q bonds may be significantly different from this value. However, as a rough estimation, using this value for both the p and q bonds and setting $s = -1$, we obtain $\beta^2 / (4\gamma) = 0.05$ eV. In the present case, $|\beta|$ is very large because the contributions from all the p and q bonds are negative as a result of the collective nature of the excitation. Since α is close to zero near the phase boundary, the ferroelectric phase is realized near the phase boundary.

From the same discussion, we can show that $|\psi^{(1)}(\tau)\rangle$ when the light is polarized to the a -direction, is hybridized to

$|\psi_0\rangle$ when the dimers denoted by I (II) in Fig. 1 shift to up (down). However, in this case, the excitation energy does not become zero at the phase boundary, and therefore the ferroelectric ground state may not be realized by the lattice motion even near the phase boundary.

As mentioned in Sec. III C, the dimer Mott insulators with alternating interdimer bond orders have an electric dipole on a dimer in the one-dimensional case. However, this is not a ferroelectric state because neighboring electric dipoles are oriented in the opposite directions as seen from Fig. 4. The two-dimensional triangle lattice is essential for the ferroelectricity.

With using the effective Hamiltonian where the interdimer part is treated perturbatively, the ferroelectric ground state is obtained without lattice deformation in Ref. 27. In Ref. 27, it is assumed that $\beta_p = \beta_{b2}$ and $\beta_q = 0$, and they find the ferroelectric ground state in the region $\beta_p / \beta_{b1} \geq 0.9$, where dimerization is very weak. In the weak dimerization region, we calculate the ground state within the present model with using the Coulomb parameters used in the paper. The ground state is the PM state, and the ferroelectric phase arising from a electric dipole on a dimer is not obtained. We consider that this is because the interdimer part cannot be treated perturbatively, especially in the weak dimerization region. The effective Hamiltonian for the strong correlation case is also proposed.²⁸

As mentioned in this subsection, some interdimer phonon modes are strongly coupled with the collective modes presented in this paper near the phase boundary of the dimer Mott transition. However, except for the region very close to the phase boundary, the excitation energies of the collective modes are much larger than those of the phonon modes, which are observed in the energy range between 2 meV to 14 meV.²⁹ Therefore, these collective modes can be regarded as electronic mode in the region.

IV. DISCUSSION

As a result of electronic degrees of freedom in a dimer, weak charge disproportion is coupled with the interdimer

bond order alternation. Although there exist collective modes which accompany bond order alternation in the simple Mott insulators, they are not photoactive. Therefore, such low-energy charge excitations do not exist in the Mott insulators. Furthermore, these collective modes are formed irrespective of the AF spin order and the Mott insulating phase. It is proposed that strong spin frustration induces charge disproportion.³⁰ However, spin frustration also does not play an important role for these modes as seen from the fact that these modes exist in the one-dimensional system with no spin frustration. This is consistent with the fact that the dielectric anomaly is observed not only in κ -(BEDT-TTF)₂Cu₂(CN)₃ but also in β' -(BEDT-TTF)₂ICl₂.¹¹ The formation of dimer and strong correlation effects are essential for these modes.

Based on the present results, the dielectric anomaly observed in κ -(BEDT-TTF)₂Cu₂(CN)₃ and β' -(BEDT-TTF)₂ICl₂ may be explained in the following way. As the temperature T is decreased, the system becomes close to the phase boundary of the dimer Mott transition and the energy difference between the dimer Mott phase and the ferroelectric phase becomes smaller. As a result, the ferroelectric domains are generated by thermal fluctuations for $T < 60$ K, which results in the broad peak with relaxor like relaxation in dielectric constant. Around $T = 6$ K, the ground state becomes ferroelectric, and this is the origin of the anomaly of various physical quantities.^{7-9,31,32} In particular, the present result is consistent with the unexpected experimental result that anomalous lattice response is observed only along the a direction.^{31,32} Similar scenarios are proposed also in Refs. 27 and 29.

ACKNOWLEDGMENTS

This research was partly supported by the Japan Society for the Promotion of Science, Grant-in-Aid for Scientific Research (C) Grant No. 19540340. The authors would like to thank M. Ikenaga and Y. Hiragi for the calculation of the ground state properties.

¹T. Sasaki, I. Ito, N. Yoneyama, N. Kobayashi, N. Hanasaki, H. Tajima, T. Ito, and Y. Iwasa, *Phys. Rev. B* **69**, 064508 (2004).

²F. Kagawa, K. Miyagawa, and K. Kanoda, *Nature (London)* **436**, 534 (2005).

³D. Faltermeier, J. Barz, M. Dumm, M. Dressel, N. Drichko, B. Petrov, V. Semkin, R. Vlasova, C. Mezère, and P. Batail, *Phys. Rev. B* **76**, 165113 (2007).

⁴T. Sasaki, N. Yoneyama, Y. Nakamura, N. Kobayashi, Y. Ike-moto, T. Moriwaki, and H. Kimura, *Phys. Rev. Lett.* **101**, 206403 (2008).

⁵M. Dumm, D. Faltermeier, N. Drichko, M. Dressel, C. Mézière, and P. Batail, *Phys. Rev. B* **79**, 195106 (2009).

⁶M. S. Nam, A. Ardavan, S. J. Blundell, and A. Schlueter, *Nature (London)* **449**, 584 (2007).

⁷Y. Shimizu, K. Miyagawa, K. Kanoda, M. Maesato, and G.

Saito, *Phys. Rev. Lett.* **91**, 107001 (2003).

⁸S. Yamashita, Y. Nakazawa, M. Oguni, Y. Oshima, H. Nojiri, Y. Shimizu, K. Miyagawa, and K. Kanoda, *Nat. Phys.* **4**, 459 (2008).

⁹M. Yamashita, N. Nakata, Y. Kasahara, T. Sasaki, N. Yoneyama, N. Kobayashi, S. Fujimoto, T. Shibauchi, and Y. Matsuda, *Nat. Phys.* **5**, 44 (2009).

¹⁰Y. Kawakami, S. Iwai, T. Fukatsu, M. Miura, N. Yoneyama, T. Sasaki, and N. Kobayashi, *Phys. Rev. Lett.* **103**, 066403 (2009).

¹¹M. Abdel-Jawad, I. Terasaki, T. Sasaki, N. Yoneyama, N. Kobayashi, Y. Uesu, and C. Hotta [arXiv:1003.3902](https://arxiv.org/abs/1003.3902) (unpublished).

¹²P. Monceau, F. Ya. Nad, and S. Brazovskii, *Phys. Rev. Lett.* **86**, 4080 (2001).

¹³N. Ikeda, H. Ohsumi, K. Ohwada, K. Ishii, T. Inami, K. Kakurai, Y. Murakami, K. Yoshii, S. Mori, Y. Horibe, and H. Kito, *Nature*

- (London) **436**, 1136 (2005).
- ¹⁴A. Nagano, M. Naka, J. Nasu, and S. Ishihara, *Phys. Rev. Lett.* **99**, 217202 (2007).
- ¹⁵M. Naka, A. Nagano, and S. Ishihara, *Phys. Rev. B* **77**, 224441 (2008).
- ¹⁶K. Yamamoto, S. Iwai, S. Boyko, A. Kashiwazaki, F. Hiramatsu, C. Okabe, N. Nishi, and K. Yakushi, *J. Phys. Soc. Jpn.* **77**, 074709 (2008).
- ¹⁷H. Kishida, H. Takamatsu, K. Fujinuma, and H. Okamoto, *Phys. Rev. B* **80**, 205201 (2009).
- ¹⁸T. Mori, H. Mori, and S. Tanaka, *Bull. Chem. Soc. Jpn.* **72**, 179 (1999).
- ¹⁹H. Kino and H. Fukuyama, *J. Phys. Soc. Jpn.* **64**, 2726 (1995).
- ²⁰H. Kino and H. Fukuyama, *J. Phys. Soc. Jpn.* **65**, 2158 (1996).
- ²¹S. Miyashita and K. Yonemitsu, *Phys. Rev. B* **75**, 245112 (2007).
- ²²S. Miyashita and K. Yonemitsu, *J. Phys. Soc. Jpn.* **77**, 094712 (2008).
- ²³T. Mori, *Bull. Chem. Soc. Jpn.* **73**, 2243 (2000).
- ²⁴R. T. Clay, S. Mazumdar, and D. K. Campbell, *Phys. Rev. B* **67**, 115121 (2003).
- ²⁵M. Kuwabara, H. Seo, and M. Ogata, *J. Phys. Soc. Jpn.* **72**, 225 (2003).
- ²⁶Y. Otsuka, H. Seo, Y. Motome, and T. Kato, *J. Phys. Soc. Jpn.* **77**, 113705 (2008).
- ²⁷M. Naka and S. Ishihara, *J. Phys. Soc. Jpn.* **79**, 063707 (2010).
- ²⁸C. Hotta, [arXiv:0912.3674](https://arxiv.org/abs/0912.3674) (unpublished).
- ²⁹K. Itoh, H. Nakaya, Y. Kawakami, T. Fukatsu, and H. Itoh, S. Iwai, T. Sasaki, and S. Saito (unpublished).
- ³⁰H. Li, R. T. Clay, and S. Mazumdar, *J. Phys.: Condens. Matter* **22**, 272201 (2010).
- ³¹M. de Souza, A. Brühl, Ch. Strack, B. Wolf, D. Schweitzer, and M. Lang, *Phys. Rev. Lett.* **99**, 037003 (2007).
- ³²R. S. Manna, M. de Souza, A. Brühl, J. A. Schlueter, and M. Lang, *Phys. Rev. Lett.* **104**, 016403 (2010).